Delayed Effects of a Single Dose Whole-Brain Radiation Therapy on Glucose Metabolism and Myelin Density

Parente, Andrea; Scandiuzzi Maciel, Elisa; J O Dierckx, Rudi A; Langendijk, Johannes A; de Vries, Erik F J; Doorduin, Janine

Published in:
International Journal of Radiation Biology

DOI:
10.1080/09553002.2020.1787542

Publication date:
2020

International Journal of Radiation Biology

ISSN: (Print) (Online) Journal homepage: https://www.tandfonline.com/loi/irab20

Delayed effects of a single-dose whole-brain radiation therapy on glucose metabolism and myelin density: a longitudinal PET study

Andrea Parente , Elisa Scandiuzzi Maciel , Rudi A. J. O. Dierckx , Johannes A. Langendijk , Erik F. J. de Vries & Janine Doorduin

To cite this article: Andrea Parente , Elisa Scandiuzzi Maciel , Rudi A. J. O. Dierckx , Johannes A. Langendijk , Erik F. J. de Vries & Janine Doorduin (2020) Delayed effects of a single-dose whole-brain radiation therapy on glucose metabolism and myelin density: a longitudinal PET study, International Journal of Radiation Biology, 96:9, 1135-1143, DOI: 10.1080/09553002.2020.1787542

To link to this article: https://doi.org/10.1080/09553002.2020.1787542

INTERNATIONAL JOURNAL OF RADIATION BIOLOGY
2020, VOL. 96, NO. 9, 1135–1143
https://doi.org/10.1080/09553002.2020.1787542

Taylor & Francis
Taylor & Francis Group

ORIGINAL ARTICLE

Delayed effects of a single-dose whole-brain radiation therapy on glucose metabolism and myelin density: a longitudinal PET study

Andrea Parente[a], Elisa Scandiuzzi Maciel[a], Rudi A. J. O. Dierckx[a], Johannes A. Langendijk[b], Erik F. J. de Vries[a], and Janine Doorduin[a]

[a]Department of Nuclear Medicine and Molecular Imaging, Medical Imaging Center, University Medical Center Groningen, University of Groningen, Groningen, The Netherlands; [b]Department of Radiation Oncology, University Medical Center Groningen, University of Groningen, Groningen, The Netherlands

ABSTRACT

Purpose: Radiotherapy is an important treatment option for brain tumors, but the unavoidable irradiation of normal brain tissue can lead to delayed cognitive impairment. The mechanisms involved are still not well explained and, therefore, new tools to investigate the processes leading to the delayed symptoms of brain irradiation are warranted. In this study, positron emission tomography (PET) is used to explore delayed functional changes induced by brain irradiation.

Materials and methods: Male Wistar rats were subjected to a single 25-Gy dose of whole brain X-ray irradiation, or sham-irradiation. To investigate delayed effects of radiation on cerebral glucose metabolism and myelin density, ^{18}F-fluorodeoxyglucose (^{18}F-FDG) PET scans were performed at baseline and on day 64 and 94, whereas N-^{11}C-methyl-4,4′-diaminostilbene (^{11}C-MeDAS) PET scans were performed at baseline and on day 60 and 90 post-irradiation. In addition, the open field test (OFT) and novel spatial recognition (NSR) test were performed at baseline and on days 59 and 89 to investigate whether whole brain irradiation induces behavioral changes.

Results: Whole-brain irradiation caused loss of bodyweight and delayed cerebral hypometabolism, with ^{18}F-FDG uptake in all brain regions being significantly decreased in irradiated rat on day 64 while it remained unchanged in control animals. Only amygdala and cortical brain regions of irradiated rats still showed reduced ^{18}F-FDG uptake on day 94. ^{11}C-MeDAS uptake in control animals was significantly lower on days 60 and 90 than at the baseline, suggesting a reduction in myelin density in young adults. In irradiated animals, ^{11}C-MeDAS uptake was similarly reduced on day 60, but on day 90 tracer uptake was somewhat increased and not significantly different from baseline anymore. Behavioral tests showed a similar pattern in control and irradiated animals. In both groups, the OFT showed significantly reduced mobility on days 59 and 89, whereas the NSR did not reveal any significant changes in spatial memory over time. Interestingly, a positive correlation between the NSR and ^{11}C-MeDAS uptake was observed in irradiated rats.

Conclusions: Whole-brain irradiation causes delayed brain hypometabolism, which is not accompanied by white matter loss. Irradiated animals showed similar behavioral changes over time as control animals and, therefore, cerebral hypometabolism could not be linked to behavioral abnormalities. However, spatial memory seems to be associated with myelin density in irradiated rats.

Abbreviations: ^{11}C-MeDAS: *N*-^{11}C-methyl-4,4′-diaminostilbene; ^{18}F-FDG: ^{18}F- fluorodeoxyglucose; GEE: Generalized estimating equations model; %ID/g: Percentage of injected dose per gram tissue; NSR: Novel spatial recognition; OFT: Open field test; PET: Positron emission tomography; PI: Preference index; SEM: Standard error of mean; VOIs: Volumes of Interest; WBRT: Whole-brain radiation therapy

ARTICLE HISTORY
Received 7 October 2019
Revised 10 April 2020
Accepted 1 June 2020

KEYWORDS
Whole-brain radiation therapy; brain injury; glucose metabolism; demyelination; positron emission tomography

Introduction

Whole-brain radiation therapy (WBRT) is an important treatment option for extensive intracranial metastases as well as prophylactic treatment for breast and lung cancer patients with high risk for developing brain metastases. However, the treatment comes with a risk: brain irradiation can lead to impairment of brain function. This has become even more relevant with the improvement of modern treatment techniques, since more patients survive long enough to show the delayed consequences of the therapy (Roman and Sperduto 1995; Chang et al. 2009; Greene-Schloesser et al. 2012). Moreover, with emerging radiation techniques like pencil beam scanning proton therapy, it becomes possible to significantly reduce brain dose to normal tissue in primary brain tumors treated with local irradiation.

CONTACT Erik F. J. de Vries e.f.j.de.vries@umcg.nl Department of Nuclear Medicine and Molecular Imaging, University of Groningen, University Medical Center Groningen, P.O. Box 30.001, Groningen, 9700 RB, The Netherlands

Supplemental data for this article is available online at here.

Radiation-induced brain injury is characterized by memory, attention and executive function loss (Balentova and Adamkov 2015). Based on the time of appearance, symptoms can be divided in acute (1st month), early-delayed (till 4th–6th month) and late-delayed toxicity (from 4th to 6th month) (Tofilon and Fike 2000; Greene-Schloesser et al. 2013). The acute and early-delayed symptoms are usually reversible, whereas the late-delayed symptoms are often irreversible. Late-delayed effects often include cognitive impairment, which can deeply affect the patient's quality of life (Liu et al. 2009; Lombardi et al. 2018; Reddy et al. 2018). The mechanisms related to delayed effects of brain irradiation are still not completely elucidated. However, in vivo MRI studies have suggested that changes in white matter are part of this process (Fujii et al. 2006; Sabsevitz et al. 2013; Nieman et al. 2015) and can possibly lead to necrosis (Furuse et al. 2015). Non-invasive in vivo imaging techniques to assess the processes associated with the late-delayed effects of brain irradiation in patients could help to improve our understanding of the mechanisms involved and facilitate improvement of treatment planning.

Positron emission tomography (PET) is a molecular imaging technique for functional assessment of biochemical and physiological processes. In this study, we used PET to assess the late-delayed changes in white matter after WBRT, using ^{11}C-MeDAS as a tracer for myelin density and ^{18}F-FDG as a tracer for brain glucose metabolism. Demyelination is directly related to the white matter damage after WBRT (Burns et al. 2016; Torrens et al. 2016; Li et al. 2018), whereas glucose metabolism could be considered a surrogate marker for neurodegeneration. The tracer ^{11}C-MeDAS has previously successfully been used for PET imaging of myelin loss and regeneration in various rodent models for multiple sclerosis (Wu et al. 2010, 2013; de Paula Faria et al. 2014a, 2014b, 2014c; Faria et al. 2014). ^{11}C-MeDAS uptake as measured *in-vivo* with PET showed a good correlation with postmortem Luxol Fast Blue histochemistry for myelin density. To evaluate behavioral changes, we used the open field test (OFT) and novel spatial recognition (NSR) test (Sun et al. 2016).

Materials and methods

Animals

Male Wistar rats (7 ± 2 weeks old, 233–308 g) were purchased from Harlan (The Netherlands). The rats were individually housed in a room with a constant temperature (21 ± 2 °C) and light/dark cycle (12:12 h). Since irradiated animals can develop a series of clinical signs of illness (e.g. damage of the skull or oral cavity, leading to disorders in eating and weight loss), a special protocol for their care was applied to reduce discomfort, starting 3 days prior to the irradiation procedure and lasting for 4 weeks. The protocol included high energy and moist diet, addition of sucrose to drinking water and smearing cream on the skin in case of hair loss. The teeth of the rats were checked weekly and cut when necessary. The special diet and the 1% of sucrose in water were also applied to the control group to avoid any bias. The animal's body weight was measured daily. All of the animal experiments were performed in accordance to the Dutch Experimental Animals Act, approved by the Institutional Animal Care and Use Committee of the University of Groningen (DEC 6158B).

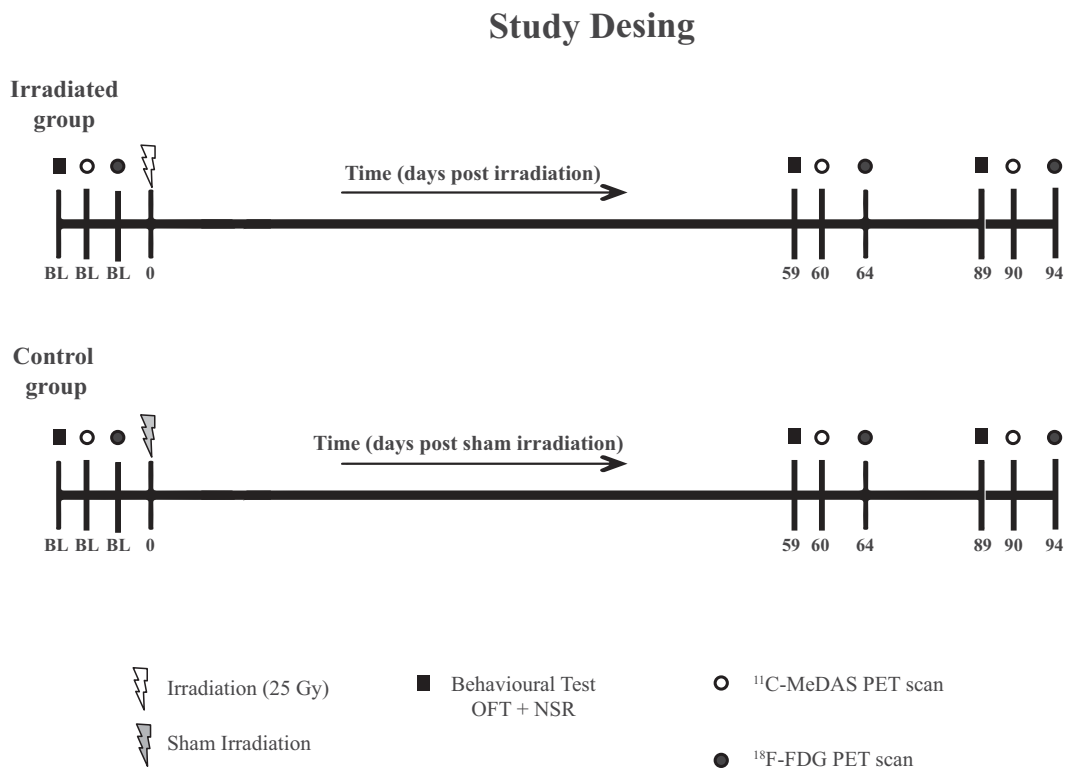

Figure 1. Study design. The time points indicate the number of days after (sham-)irradiation. BL: baseline; OFT: open field test; NSR: novel spatial recognition test.

Study design

Figure 1 summarizes the overall design of the study. Experimental animals ($n = 8$) were submitted to irradiation (25 Gy) on day 0. ^{18}F-FDG PET scans were performed before whole-brain irradiation (baseline) scan and on days 64 and 94 post-irradiation. ^{11}C-MeDAS PET scans were performed at baseline and on days 60 and 90 post-irradiation. OFT and NSR test were performed at baseline and on 59 and 89 days post-irradiation. One of the irradiated animals died between 2 and 3 months after the irradiation procedure and, therefore, did not undergo the PET scans or behavioral tests at the 3 months' time point.

During this longitudinal study, we realized that aging might have an effect on the results (Chen et al. 2011; Mengler et al. 2014). Therefore, a group of control animals ($n = 8$) were added later to the study. Consequently animals were not randomized. Control animals were handled similarly as experimental animals, but were submitted to sham-irradiation (X-ray apparatus remained switched-off).

Whole-brain irradiation procedure

The procedure was performed using a self-contained X-ray irradiator for small animals (X-RAD 320, Precision X-ray – Pxi, Austin, TX). Rats were anesthetized with an intraperitoneal injection of ketamine (25 mg/kg) and medetomidine (0.2 mg/kg). The whole rat brain was then irradiated with 25 Gy of X-rays. A whole brain lead collimator with tight margins around the brain was designed, based on MRI scans of five animals. The collimator was constructed in such a way that critical structures, such as the eyes, the parotid and tear glands, were shielded during the irradiation procedure (Supplementary Figure 1).

PET acquisition

The ^{18}F-FDG PET scans were performed in the morning (always between 8:00 h and 10:30 h) using a small animal PET camera (Focus 220, Siemens Medical Solutions, Ann Arbor, MI). In anesthetized animals, brain glucose metabolism – and, thus, ^{18}F-FDG uptake – is low. ^{18}F-FDG (22.5 ± 0.9 MBq) was, therefore, injected intraperitoneally in conscious animals to allow for tracer distribution while the brain of the animal is active, according to the standard procedure in our institution (de Paula Faria et al. 2014b; Vállez García et al. 2016; Kopschina Feltes et al. 2019). It has previously been reported that intraperitoneal and intravenous injection of ^{18}F-FDG give similar brain uptake at late time points (Schiffer et al. 2007; Wong et al. 2011). Rats were put back in their cage for 40 min. Then, rats were anesthetized with an isoflurane and oxygen mixture (5% induction, 1.8–2% maintenance, 0.8 L/min) and positioned in the PET camera in a supine position with their heads in the center of the field of view. Before the start of the scan, a drop of blood was taken from the tail vein to determine blood glucose levels using a glucose meter (Johnson & Johnson). The glucose measurement was performed in triplicate using different strips (Deleye et al. 2014). A 30-min static emission scan was acquired, starting 45 min after tracer injection. After the acquisition of the emission scan was complete, a 515 s transmission scan for attenuation and scatter correction was obtained using a ^{57}Co point source.

The ^{11}C-MeDAS PET scans were performed in the early afternoon. Since myelin density is not dependent on brain activity, ^{11}C-MeDAS could be injected intravenously in anesthetized animals. Rats were anesthetized with an isoflurane and oxygen mixture (5% induction, 2% maintenance, 0.8 L/min). ^{11}C-MeDAS (45.4 ± 4.4 MBq) was injected via the penile vein. After injection, the rats were kept under light anesthesia (1.5%) to enable tracer distribution, according to the previously described procedure (de Paula Faria et al. 2014a, 2014b). After 30 min, the rats were placed in the PET camera in a supine position with their heads in the center of the field of view. A transmission scan was obtained using a ^{57}Co point source for attenuation and scatter correction. Thirty minutes after tracer injection, a 30-min static emission scan was acquired.

During the PET scans, heart rate and O_2 saturation were monitored, body temperature was maintained using heating pads and eye salve was applied to prevent conjunctival dehydration.

PET reconstruction

PET scans were reconstructed iteratively (OSEM2D, 4 iterations, and 16 subsets) into a single frame of 30 min after being normalized and corrected for attenuation, scatter and decay of radioactivity. The scans were quantitatively analyzed using PMOD 3.8 software (PMOD Technologies, Zürich, Switzerland). For this purpose, the reconstructed scans were automatically registered with a reference tracer template (Vállez Garcia et al. 2015). Volumes of Interest (VOIs) were transferred from the template to the co-registered PET images and tracer uptake in these VOIs was measured. VOIs were selected taking the size of brain regions and camera resolution into consideration. Therefore, the following brain regions were selected for investigation: whole brain, hippocampus, hypothalamus, thalamus, striatum, amygdala, midbrain, brainstem, cerebellum, frontal cortex, temporal cortex, and parietal/occipital cortex.

^{18}F-FDG and ^{11}C-MeDAS radioactivity concentrations were determined for each VOI and converted into the percentage of injected dose per gram of tissue (%ID/g), which is defined as

(Radioactivity concentration in tissue [Bq/cm^3] × 100%)/(Injected dose [Bq]).

It was assumed that 1 cm^3 of brain tissue equals 1 g. The ^{18}F-FDG uptake was corrected for blood glucose levels (Woo et al. 2008; Deleye et al. 2014), according to the formula: $\%ID/g_{corr}$ = [%ID/g X blood glucose (mol/L)/5.55 (mol/L)].

One irradiated animal died on day 79 and therefore PET scans on day 90/94 could not be acquired for this animal. Due to technical problems with the tracer injection (injection in intestines, extravasation), four ^{18}F-FDG PET scans

(baseline: 1 irradiated, 2 controls; day 94: 1 control) and one ^{11}C-MeDAS PET scan (day 90: 1 control) were excluded from the analysis.

Open field test

Animals were allowed to acclimatize in the experimental room for at least 1 h. The test was always performed between 8:00 and 9:00 AM. The rats were placed in an elliptical arena (126 × 88 × 60 cm) and their locomotor behavior was recorded on video for 5 min. The total distance moved was analyzed using Ethovision XT8.5 software (Noldus Information Technology, Wageningen, The Netherlands). The arena was cleaned with 70% ethanol after each session to avoid bias due to other animal's odors.

Novel spatial recognition

The test was always performed 1 h after the OFT. The rats were placed in a square arena (40 × 40 × 44 cm). Two objects were placed in this arena and the rats were allowed to explore for 5 min and then returned to their home cage. After 90 min, the rats were again placed in the same arena, only this time, one of the objects was moved to a different position (Roozendaal et al. 2010). The behavior of the rats was then recorded on video for 5 min. The time the animals spent exploring each object was measured and the Preference Index (PI) (Ennaceur and Delacour 1988; Antunes and Biala 2012) was calculated by dividing the time spent exploring the object in a new position by the total time exploring both objects. The object that changed positions had to be explored for at least 2.5 s in both the familiarization and testing phase, and the object that remained in the same place had to be explored for at least 1 s in the test phase. The animals that did not reach these cut off values were excluded from the analysis. Thus, final analysis was performed on $n = 6$ (baseline; day 59), or $n = 5$ (day 89) in the control group and on $n = 6$ (baseline; day 89), or $n = 5$ (day 59) in the irradiated group. The arena and the objects were cleaned with 70% ethanol after each session to avoid bias due to other animal's odors.

Statistical analysis

All statistical tests were performed using SPSS 23 software (IBM Corporations, Armonk, NY). The generalized estimating equations (GEE) model can account for missing data and longitudinal analysis and was, therefore, used for within group comparison of tracer uptake in each brain region, the total distance moved in the OFT, the PI in the NSR test and the change in bodyweight. For all parameters, within-group analysis of the longitudinal effects of whole-brain irradiation was performed, using the GEE model. The GEE model was also used for between-group comparison of bodyweight and behavior, but not for between-group comparison of PET data, due to unexpected significant baseline differences in ^{18}F-FDG and ^{11}C-MeDAS uptake between control and irradiated animals. The independent structure was the best working correlation matrix based on the quasi-likelihood under the independence model information criterion value. Post-hoc Bonferroni correction was applied to correct for multiple comparisons and the associated p values were considered significant when $p < .05$.

Results

Bodyweight

Bodyweight was measured daily to assess the effect of brain irradiation in the acute and delayed phase (Figure 2). Statistically significant ($p < .001$) effects were observed in the GEE analysis for the factors 'time' and 'group'. The control group showed a gradual increase in bodyweight over time. The 25-Gy group, however, showed a continuous weight loss during the first 10 days (−13%) compared to day 0, and a subsequent weight gain, without reaching the bodyweight of the control group until the end of the experiment. Irradiation caused a significant reduction in bodyweight, as compared to controls ($p < .001$) from day 5 post-irradiation onward. Between days 37 and 45, the irradiated rats revealed a small period of bodyweight decrease (−4.2%), which could be due to eating problems caused by overgrowth of the upper incisors. After the upper incisors were cut, the bodyweight slowly increased until day 59. Then, there was a transient reduction in bodyweight until day 64 (−6.7%), followed by a slow increase until day 78 post-irradiation. We observed that the animals developed mucositis in the oral cavity about 2 months after radiotherapy, which could explain the second transient drop in bodyweight (Maria et al. 2017).

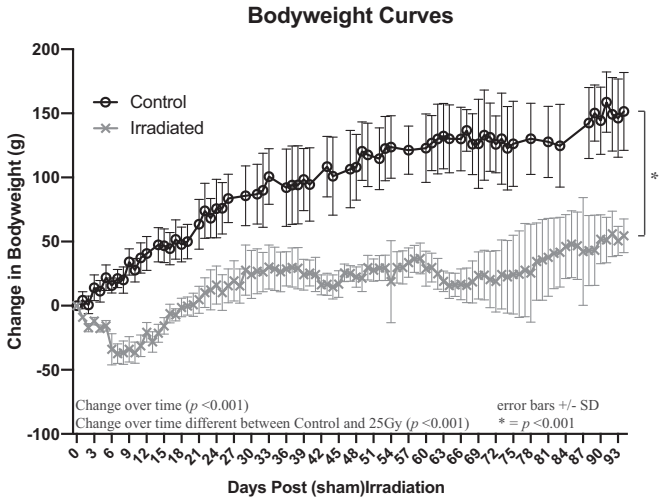

Figure 2. Average bodyweight change (g) from baseline ([bodyweight at specific time point] – [bodyweight at baseline]) from (sham-)irradiation until termination ($n = 8$, one irradiated rat died on day 79). Irradiated animals do not gain weight in the same way as control animals. Statistical analysis (GEE model) showed a significant effect of time on bodyweight and a significant interaction between group and time. No statistically significant differences between groups were observed from baseline until day 5 post-irradiation. From day 5 until the end of the study, the bodyweight of irradiated animals was significantly lower than controls ($p < .001$).

^{18}F-FDG PET

In the control group, neither the whole brain nor any individual brain region showed significant changes in ^{18}F-FDG uptake over time. In the irradiated group, there was significant decrease in ^{18}F-FDG uptake (%ID/g_{corr}) in whole brain (24%, $p < .001$) and in all individual brain regions (17–27%, $p < .01$ or $< .001$) between baseline and day 64. On day 94, however, ^{18}F-FDG uptake in all brain regions tended to increase a bit again as compared to day 64 (3–9%), although this increase was not statistically significant. Consequently, only the whole brain (19%, $p < .05$), cortical areas and amygdala (22–24%) still showed significantly lower ^{18}F-FDG uptake on day 94 than at baseline (Figure 3, Table 1).

^{11}C-MeDAS PET

In the control group, ^{11}C-MeDAS uptake in the whole brain and all specific brain regions significantly decreased (13–23%, $p < .001$) between baseline and day 60. Between days 60 and 90, tracer uptake remained unchanged and, therefore, ^{11}C-MeDAS uptake at day 90 was also significantly lower than at baseline (15–23%, $p < .001$). In the irradiated group, ^{11}C-MeDAS uptake in the whole brain and all specific brain regions also showed a significant decrease (18–24%, $p < .001$) between baseline and day 60. However, ^{11}C-MeDAS uptake in irradiated animals tended to increase again between days 60 and 90. As a result, the difference in ^{11}C-MeDAS uptake between baseline and day 90 was no longer statistically significant ($p > .05$) anymore in the whole brain or any brain region, except in the amygdala (−18%, p .04) (Figure 4, Table 2).

Open field test

The motor activity was evaluated by the total distance the animals moved in the OFT. The results are summarized in Figure 5(a). Within-group analyses indicated that control and irradiated animals behaved in the same way. Both groups showed a significant decrease ($p < .001$) in total ambulatory distance between baseline and day 59 and baseline and day 89, but no significant differences between days

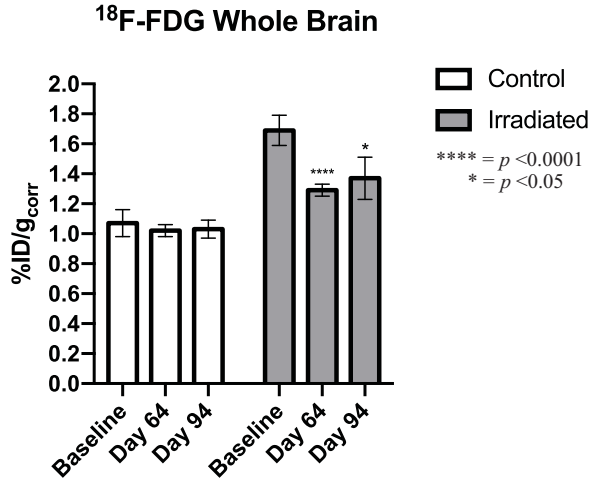

Figure 3. Results of ^{18}F-FDG PET imaging of whole-brain glucose metabolism in control animals (white bars) and irradiated rats (gray bars) at several time points after whole-brain irradiation with 25 Gy of X-rays. Tracer uptake is expressed as %ID/g corrected for blood glucose (mean ± SEM). Control group: $n = 6$ (baseline), $n = 7$ (day 94), or $n = 8$ (day 64). Irradiated group: $n = 7$ (baseline; day 94), or $n = 8$ (day 64). Significant differences are relative to baseline values in the same group, and are indicated by $^{*}p < .05$ and $^{****}p < .0001$.

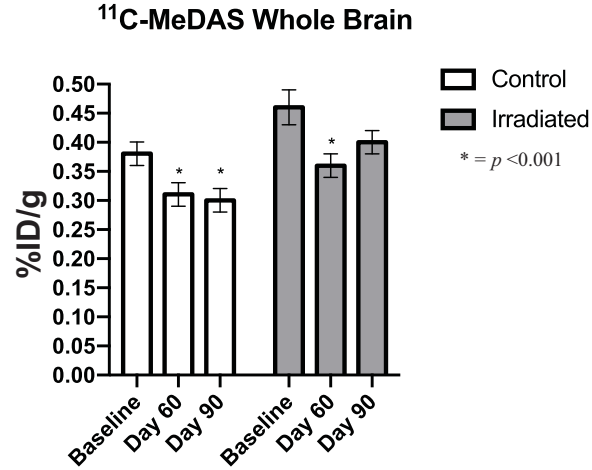

Figure 4. Results of ^{11}C-MeDAS PET imaging of whole brain myelination in control animals (white bars) and irradiated rats (gray bars) at several time points after whole-brain irradiation with 25 Gy of X-rays. Tracer uptake is expressed as %ID/g (mean ± SEM). Control group: $n = 7$ (day 94), or $n = 8$ (baseline; day 64). Irradiated group: $n = 7$ (day 94), or $n = 8$ (baseline; day 64). Significant differences are relative to baseline values in the same group, and are indicated by $^{*}p < .001$.

Table 1. 18F-FDG uptake, expressed as %ID/g_{corr} (mean ± SEM), in various brain regions of irradiated and control rats.

Group →	CTRL			25 Gy irradiated		
Time point →	Baseline ($n = 6$)	Day 64 ($n = 8$)	Day 94 ($n = 7$)	Baseline ($n = 7$)	Day 64 ($n = 8$)	Day 94 ($n = 7$)
Amygdala	1.06 ± 0.10	0.99 ± 0.04	0.99 ± 0.05	1.62 ± 0.10	1.23 ± 0.03*	1.27 ± 0.12^
Brainstem	1.07 ± 0.11	1.04 ± 0.04	1.04 ± 0.06	1.58 ± 0.08	1.30 ± 0.05^	1.37 ± 0.13
Cerebellum	0.93 ± 0.08	0.92 ± 0.04	0.92 ± 0.06	1.49 ± 0.08	1.21 ± 0.04*	1.32 ± 0.12
Frontal cortex	1.05 ± 0.07	1.04 ± 0.05	1.06 ± 0.06	1.77 ± 0.10	1.27 ± 0.05*	1.38 ± 0.14^
Hippocampus	1.19 ± 0.10	1.11 ± 0.05	1.13 ± 0.06	1.89 ± 0.13	1.42 ± 0.05*	1.51 ± 0.16
Hypothalamus	1.01 ± 0.12	0.97 ± 0.04	0.97 ± 0.06	1.47 ± 0.09	1.21 ± 0.05^	1.24 ± 0.14
Midbrain	1.20 ± 0.11	1.14 ± 0.05	1.15 ± 0.07	1.82 ± 0.11	1.50 ± 0.05^	1.60 ± 0.16
Parietal occipital cortex	1.10 ± 0.08	1.04 ± 0.04	1.06 ± 0.06	1.75 ± 0.10	1.27 ± 0.04*	1.36 ± 0.14^
Striatum	1.31 ± 0.11	1.21 ± 0.05	1.24 ± 0.07	2.03 ± 0.13	1.57 ± 0.06*	1.61 ± 0.20
Temporal cortex	1.14 ± 0.10	1.10 ± 0.04	1.09 ± 0.06	1.73 ± 0.08	1.30 ± 0.04*	1.32 ± 0.13^
Thalamus	1.27 ± 0.11	1.21 ± 0.06	1.23 ± 0.07	1.97 ± 0.12	1.56 ± 0.06*	1.69 ± 0.19
Whole brain	1.07 ± 0.09	1.02 ± 0.04	1.03 ± 0.06	1.69 ± 0.10	1.29 ± 0.04*	1.37 ± 0.14#

^{18}F-FDG uptake (%ID/g_{corr}) in control rats and rats exposed to a single 25-Gy dose of whole-brain irradiation, at baseline and on days 64 and 94. The p values for the within-group analyses relative to baseline are provided: $^{*}p \leq .001$; $^{\wedge}p \leq .01$; $^{\#}p \leq .05$.

Table 2. 11C-MeDAS uptake, expressed as %ID/g (mean ± SEM), in various brain regions of control and irradiated rats.

Group →	CTRL			25 Gy irradiated		
Time point →	Baseline ($n = 8$)	Day 60 ($n = 8$)	Day 90 ($n = 7$)	Baseline ($n = 8$)	Day 60 ($n = 8$)	Day 90 ($n = 7$)
Amygdala	0.29 ± 0.01	0.24 ± 0.01*	0.23 ± 0.01*	0.34 ± 0.02	0.27 ± 0.01*	0.28 ± 0.02#
Brainstem	0.48 ± 0.03	0.42 ± 0.02*	0.41 ± 0.02*	0.56 ± 0.04	0.46 ± 0.03*	0.50 ± 0.03
Cerebellum	0.37 ± 0.02	0.31 ± 0.01*	0.30 ± 0.01*	0.45 ± 0.03	0.36 ± 0.02*	0.39 ± 0.02
Frontal cortex	0.36 ± 0.02	0.28 ± 0.02*	0.29 ± 0.02*	0.45 ± 0.03	0.36 ± 0.02*	0.40 ± 0.02
Hippocampus	0.38 ± 0.02	0.31 ± 0.01*	0.29 ± 0.01*	0.46 ± 0.03	0.36 ± 0.02*	0.40 ± 0.02
Hypothalamus	0.36 ± 0.02	0.29 ± 0.01*	0.28 ± 0.02*	0.44 ± 0.03	0.34 ± 0.02*	0.36 ± 0.02
Midbrain	0.50 ± 0.03	0.39 ± 0.02*	0.39 ± 0.02*	0.61 ± 0.04	0.47 ± 0.04*	0.53 ± 0.03
Parietal occipital cortex	0.35 ± 0.02	0.27 ± 0.01*	0.27 ± 0.02*	0.42 ± 0.03	0.32 ± 0.02*	0.55 ± 0.02
Striatum	0.43 ± 0.02	0.36 ± 0.01*	0.36 ± 0.02*	0.53 ± 0.04	0.41 ± 0.03*	0.47 ± 0.03
Temporal cortex	0.30 ± 0.02	0.24 ± 0.01*	0.24 ± 0.01*	0.36 ± 0.02	0.28 ± 0.01*	0.29 ± 0.02
Thalamus	0.46 ± 0.03	0.36 ± 0.02*	0.36 ± 0.02*	0.56 ± 0.04	0.43 ± 0.03*	0.49 ± 0.03
Whole brain	0.38 ± 0.02	0.31 ± 0.02*	0.30 ± 0.02*	0.46 ± 0.03	0.36 ± 0.02*	0.40 ± 0.02

[11]C-MeDAS uptake (%ID/g) in control rats and rats exposed to a single 25-Gy dose of whole-brain irradiation at baseline and on days 60 and 90. The p values for the within-group analysis relative to baseline are provided: *$p \leq .001$; #$p \leq .05$.

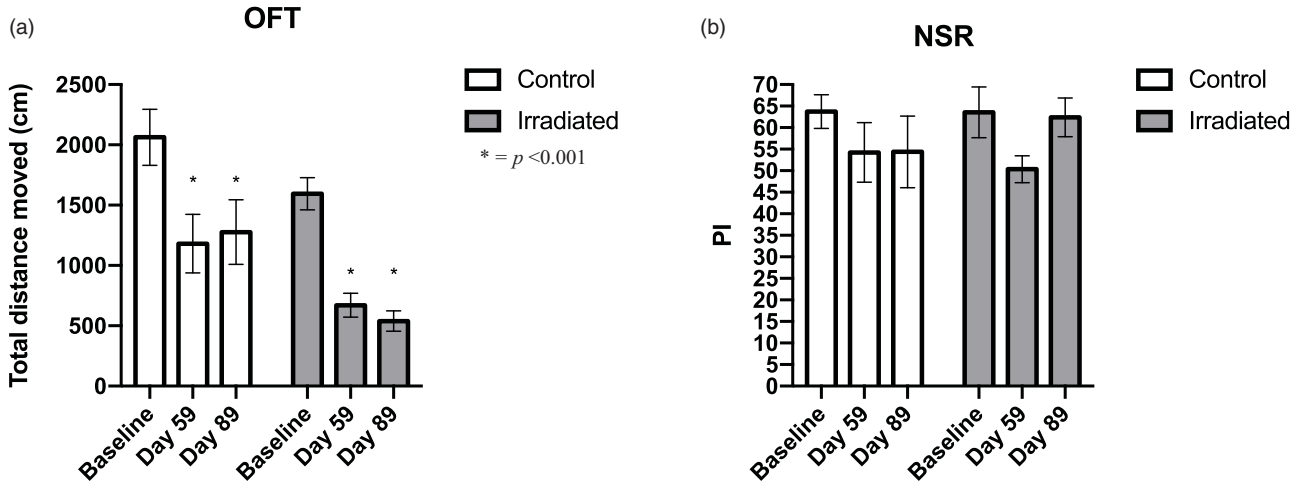

Figure 5. (a) The total distance moved in the open field test, expressed in cm (mean ± SEM; $n = 8$) ($n = 7$ for irradiated group, day 89). (b) The preference index in the novel spatial recognition test (mean ± SEM) in control animals (white bars) and irradiated rats (gray bars) at several time points after whole brain irradiation with 25 Gy of X-rays. Control group: $n = 6$ (baseline; day 59), or $n = 5$ (day 89). Irradiated group: $n = 6$ (baseline; day 89), or $n = 5$ (day 59). Significant differences are relative to baseline values in that group, and are indicated by *$p < .001$.

59 and 89. The results of the OFT did not correlate with [18]F-FDG or [11]C-MeDAS uptake.

Novel spatial recognition

The results of the NSR test are summarized in Figure 5(b). Within-group analyses indicated that both control and irradiated animals did not show any significant change in PI over time. However, a correlation between PI and whole brain [11]C-MeDAS uptake was observed. For the combined data from baseline, days 60 and 90, a significant correlation between PI and [11]C-MeDAS uptake was found in the irradiated group ($p < .002$; R^2 0.51), but not in the control group (p .92; R^2 0.0007) (Figure 6).

Discussion

To our knowledge, this is the first molecular imaging study analyzing both brain metabolism and myelin density in the delayed phase of radiation-induced brain injury. Our study

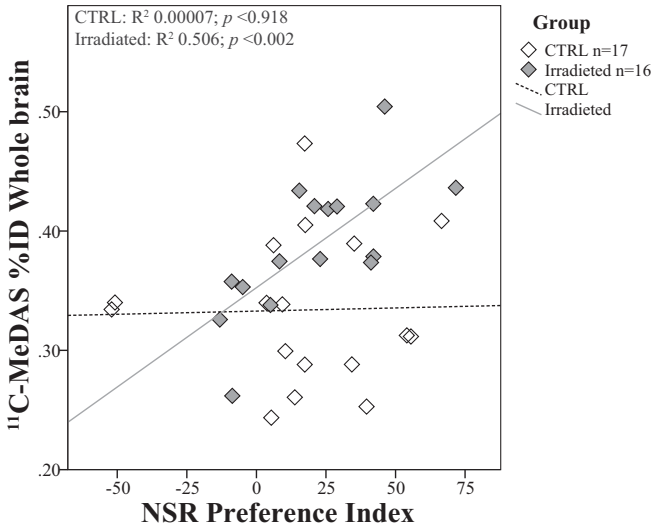

Figure 6. Correlation between [11]C-MeDAS uptake (%ID/g) in the whole brain and the preference index from the novel spatial recognition test. The results of control animals (white square) and irradiated rats (gray dots) at baseline and on day 60 and 90 after (sham-)irradiation are presented.

aimed to reveal two characteristics of delayed toxicity after whole-brain irradiation: hypometabolism and demyelination. ^{18}F-FDG PET scans showed that a single 25-Gy dose of WBRT indeed induced delayed brain glucose hypometabolism in rats. Yet, ^{11}C-MeDAS PET scans did not reveal any demyelination in the delayed phase, but rather a possible trend toward remyelination in the irradiated group. This is in line with a trend toward increased ^{18}F-FDG uptake in the inner brain areas. The OFT and NSR test did not show any radiation-induced delayed behavioral changes. However, 25-Gy brain irradiation caused alopecia in the irradiated area, damage in oral cavity and mucositis that could lead to eating problems and significant weight loss (Figure 2).

Our results show that a decrease in glucose metabolism in the whole brain and all individual brain regions started to appear 2 months after whole-brain irradiation and persisted only in amygdala and cortical areas after 3 months. Whole-brain hypometabolism induced by WBRT has also been described in another preclinical (Rana et al. 2013) and some clinical studies (Andersen et al. 2003; Clavo et al. 2009; Robbins et al. 2012; Tallet et al. 2012). The preclinical study by Rana et al. (2013), however, focused on the acute phase after radiation therapy. With proton magnetic resonance spectroscopy, they observed brain hypometabolism already 2–10 days after mice were subjected to whole-body radiation therapy. Some clinical studies (Andersen et al. 2003; Clavo et al. 2009; Robbins et al. 2012) analyzed the late-delayed effects of brain irradiation, varying from 9 months until years post-exposure. In line with our findings, these studies showed a globally decreased brain glucose metabolism, which also included the hippocampus. The hippocampus is closely involved in cognitive impairment, which is also a characteristic of late-delayed radiation toxicity. In our study, glucose metabolism in hippocampus was not more affected than other brain regions 3 months after irradiation, which might suggest damage in hippocampus was still relatively mild and could thus explain the absence of cognitive abnormalities in the NSR memory test.

In our study, the control group showed lower ^{11}C-MeDAS uptake at days 60 and 90 than at baseline, suggesting a decrease in myelin density between baseline and days 60–90. We observed a similar pattern in myelin density changes in irradiated rats as in controls, although there appeared to be a non-significant tendency toward an increase in myelin density 3 months after radiation therapy, as compared to day 60. In line with our data, previous studies suggested that demyelination after 25-Gy WBRT in rodents is a process that mainly occurs in the acute phase (Burns et al. 2016), with myelin density recovering to normal levels after around 3–6 months (Panagiotakos et al. 2007; Fu et al. 2017). This recovery is hypothesized to occur mainly due to the capacity of oligodendrocyte progenitor cells to migrate to the sites of myelin damage and remyelinate the injured white matter tracts.

In line with this hypothesis, we noticed that whole brain ^{11}C-MeDAS uptake and the NSR test showed a similar temporal pattern in the irradiated group. Regression analysis indeed confirmed that the ^{11}C-MeDAS uptake and the PI were significantly correlated in the irradiated group when all data from baseline, days 60, and 90 were pooled. This correlation suggests that changes in myelin density are associated with altered cognitive performance in spatial recognition. This finding is in line with new research that recognized that white matter is equally critical for cognition and behavior as gray matter is (Filley 2005; Fields 2008; Filley 2012; Filley and Fields 2016).

Combining all PET imaging results, our study suggests that the reduced brain glucose metabolism 3 months after whole brain irradiation is probably not due to white matter involvement (oligodendrocytes), since the myelin density seems to be normal or even slightly increased to recover damage. Therefore, our results might point toward neuronal cell death of gray matter. The delayed hypometabolism could be due to a lower global brain activity. Studies in neurodegenerative diseases such as Parkinson's and Alzheimer's disease (Zilberter and Zilberter 2017) have suggested that brain hypometabolism is preceding neurodegeneration and can be aggravated as a consequence of it. We investigated brain hypometabolism only for 3 months after WBRT and, therefore, a longer follow up may be needed to detect late neurodegeneration and the accompanying demyelination.

This study has some limitations. Most importantly, the control group was added later in time and therefore no randomization could be applied. For an unknown reason, this has led to baseline differences in the PET data between groups. The baseline differences in PET tracer uptake between groups were thoroughly investigated, but could not be explained by different tracer properties (e.g. purity, molar activity, injected mass), animal weight and age at arrival, camera characteristics, imaging procedures or quality of tracer injection. These baseline differences prompted us to perform only within-group comparisons in control and irradiated animals separately. Despite this limitation, it was still possible to detect effects of brain irradiation.

Another limitation is that we used behavioral tests in this study (OFT and NSR) that were available in our animal facility at the time of the experiment. These tests may not be the most sensitive ones to detect the kind of cognitive impairment that comes with WBRT[17]. Moreover, in the analysis of the NSR test, we had to exclude several animals due to insufficient exploration of the objects in the first exploratory round. As a result, the sample size may have been insufficient to detect significant differences and thus a larger number of animals may be needed. Finally, the 3 months of follow-up after WBRT in this study may still have been too short to capture the late-delayed adverse events caused by the treatment.

In conclusion, WBRT reduced whole-brain glucose metabolism from 2 to 3 months after treatment. This whole hypometabolism is probably not due to involvement of white matter, since the myelin levels were shown to be normal or even slightly increased at this time point. Statistically significant behavioral abnormalities could not be detected in this study, although we found correlation between myelin density and spatial memory in the irradiated group. Apart

from that, the imaging findings could not be linked to delayed symptoms. Further research is needed to elucidate the pathophysiology underlying the delayed hypometabolism. For this purpose, imaging studies to investigate the integrity of gray matter using, for example, the PET tracer ^{11}C-flumazenil may provide more insight.

Acknowledgements

The authors thank David Vállez García for his support in the statistical analysis, Alexandre Shoji for his support during the image acquisition and Peter van Luijk for his support regarding the study design.

Disclosure statement

The scholarship of Andrea Parente was financed by Siemens Medical Solutions Inc. The other authors declare no conflict of interest.

Funding

This work was supported by Siemens Medical Solutions Inc.

Notes on contributors

Andrea Parente is a PhD student at the Department of Nuclear Medicine and Molecular Imaging at University Medical Center Groningen, University of Groningen, The Netherlands. His PhD project focuses on in vivo imaging of radiotherapy-induced brain injury and evaluation of behavioral changes.

Elisa Scandiuzzi Maciel is a 5th year medical student at the Federal University of São Paulo, Escola Paulista de Medicina, in São Paulo, Brazil. She participated in the study during a research internship at the Department of Nuclear Medicine and Molecular Imaging at the University of Groningen for one year.

Rudi A. J. O. Dierckx is the Chairman of the Medical Imaging Center consisting of the department of Nuclear Medicine Molecular Imaging and the Department of Radiology at the University Medical Center Groningen in The Netherlands. He is a board certified nuclear medicine physician. His primary research interests relate to PET studies of the human brain.

Johannes A. Langendijk is the Head of the Department of Radiation Oncology of the University Medical Center Groningen in The Netherlands. His research interests are related to radiation induced normal tissue damage and complications, development of new radiation technologies and image guided radiotherapy.

Erik F. J. de Vries is a Full Professor in Translational Molecular Imaging at the department of Nuclear Medicine and Molecular Imaging of the University Medical Center Groningen, The Netherlands. His research focuses on translational PET imaging of drug targets and inflammatory processes in neuroscience and oncology.

Janine Doorduin is an Assistant Professor at the Department of Nuclear Medicine and Molecular Imaging of the University Medical Center Groningen, The Netherlands. Her research focuses on the role of neuroinflammation in psychiatric and neurological disorders, involving both preclinical and clinical PET studies.

ORCID

Andrea Parente http://orcid.org/0000-0001-6820-9474
Elisa Scandiuzzi Maciel http://orcid.org/0000-0003-4322-1260
Rudi A. J. O. Dierckx http://orcid.org/0000-0003-4971-2909
Johannes A. Langendijk http://orcid.org/0000-0003-1083-372X
Erik F. J. de Vries http://orcid.org/0000-0002-6915-1590
Janine Doorduin http://orcid.org/0000-0003-2925-9959

References

Andersen PB, Krabbe K, Leffers AM, Schmiegelow M, Holm S, Laursen H, Müller JR, Paulson OB. 2003. Cerebral glucose metabolism in long-term survivors of childhood primary brain tumors treated with surgery and radiotherapy. J Neurooncol [Internet]. 62: 305–313.

Antunes M, Biala G. 2012. The novel object recognition memory: neurobiology, test procedure, and its modifications. Cogn Process. 13:93–110.

Balentova S, Adamkov M. 2015. Molecular, cellular and functional effects of radiation-induced brain injury: a review. Int J Mol Sci. 16: 27796–27815.

Burns TC, Awad AJ, Li MD, Grant GA. 2016. Radiation-induced brain injury: low-hanging fruit for neuroregeneration. Neurosurg Focus. 40:E3.

Chang EL, Wefel JS, Hess KR, Allen PK, Lang FF, Kornguth DG, Arbuckle RB, Swint JM, Shiu AS, Maor MH, et al. 2009. Neurocognition in patients with brain metastases treated with radiosurgery or radiosurgery plus whole-brain irradiation: a randomised controlled trial. Lancet Oncol. 10:1037–1044.

Chen L, Lu W, Yang Z, Yang S, Li C, Shi X, Tang Y. 2011. Age-related changes of the oligodendrocytes in rat subcortical white matter. Anat Rec (Hoboken). 294:487–493.

Clavo B, Robaina F, Montz R, Carames MA, Lloret M, Ponce P, Hernandez MA, Carreras JL. 2009. Modification of glucose metabolism in radiation-induced brain injury areas using cervical spinal cord stimulation. Acta Neurochir. 151:1419–1425.

de Paula Faria D, de Vries EFJ, Sijbesma JWA, Buchpiguel CA, Dierckx RAJO, Copray SCVM. 2014b. PET imaging of glucose metabolism, neuroinflammation and demyelination in the lysolecithin rat model for multiple sclerosis. Mult Scler. 20:1443–1452.

de Paula Faria D, de Vries EFJ, Sijbesma JA, Dierckx RAJ, Buchpiguel CA, Copray S. 2014c. PET imaging of demyelination and remyelination in the cuprizone mouse model for multiple sclerosis: a comparison between [11C]CIC and [11C]MeDAS. Neuroimage. 87:395–402.

de Paula Faria D, Vlaming MLH, Copray S, Tielen F, Anthonijsz HJA, Sijbesma JWA, Buchpiguel CA, Dierckx R, van der Hoorn JWA, de Vries E. 2014a. PET imaging of disease progression and treatment effects in the experimental autoimmune encephalomyelitis rat model. J Nucl Med. 55:1330–1335.

Deleye S, Verhaeghe J, Wyffels L, Dedeurwaerdere S, Stroobants S, Staelens S. 2014. Towards a reproducible protocol for repetitive and semi-quantitative rat brain imaging with (18) F-FDG: exemplified in a memantine pharmacological challenge. Neuroimage. 96:276–287.

Ennaceur A, Delacour J. 1988. A new one-trial test for neurobiological studies of memory in rats. 1:behavioral data. Behav Brain Res. 31: 47–59.

Faria DdP, Copray S, Sijbesma JWA, Willemsen ATM, Buchpiguel CA, Dierckx R, de Vries E. 2014. PET imaging of focal demyelination and remyelination in a rat model of multiple sclerosis: comparison of [11C]MeDAS, [11C]CIC and [11C]PIB. Eur J Nucl Med Mol Imaging. 41:995–1003.

Fields RD. 2008. White matter matters. Sci Am. 298:42–9.

Filley CM, Fields RD. 2016. White matter and cognition: making the connection. J Neurophysiol. 116:2093–2104.

Filley CM. 2005. White matter and behavioral neurology. Ann N Y Acad Sci. 1064:162–83.

Filley CM. 2012. White matter dementia. Ther Adv Neurol Disord. 5: 267–77.

Fu Z, Zhao Y, Zhang K, Wang J, Zhang M, Zhao X. 2017. Age-dependent responses of brain myelin integrity and behavioral performance to radiation in mice. Radiat Res. 188:505–516.

Fujii O, Tsujino K, Soejima T, Yoden E, Ichimiya Y, Sugimura K. 2006. White matter changes on magnetic resonance imaging following whole-brain radiotherapy for brain metastases. Radiat Med. 24: 345–350.

Furuse M, Nonoguchi N, Kawabata S, Miyatake SI, Kuroiwa T. 2015. Delayed brain radiation necrosis: pathological review and new molecular targets for treatment. Med Mol Morphol. 48:183–190.

Greene-Schloesser D, Moore E, Robbins ME. 2013. Molecular pathways: radiation-induced cognitive impairment. Clin Cancer Res. 19: 2294–2300.

Greene-Schloesser D, Robbins ME, Peiffer AM, Shaw EG, Wheeler KT, Chan MD. 2012. Radiation-induced brain injury: a review. Front Oncol [Internet]. 2:73.

Kopschina Feltes P, de Vries EF, Juarez-Orozco LE, Kurtys E, Dierckx RA, Moriguchi-Jeckel CM, Doorduin J. 2019. Repeated social defeat induces transient glial activation and brain hypometabolism: a positron emission tomography imaging study. J Cereb Blood Flow Metab. 39:439–453.

Li H, Deng L, Bai HX, Sun J, Cao Y, Tao Y, States LJ, Farwell MD, Zhang P, Xiao B, et al. 2018. Diagnostic accuracy of amino acid and FDG-PET in differentiating brain metastasis recurrence from radionecrosis after radiotherapy: a systematic review and meta-analysis. AJNR Am J Neuroradiol. 39:280–288.

Liu R, Page M, Solheim K, Fox S, Chang SM. 2009. Quality of life in adults with brain tumors: current knowledge and future directions. Neuro-oncology. 11:330–339.

Lombardi G, Bergo E, Del Bianco P, Bellu L, Pambuku A, Caccese M, Trentin L, Zagonel V. 2018. Quality of life perception, cognitive function, and psychological status in a real-world population of glioblastoma patients treated with radiotherapy and temozolomide: a single-center prospective study. Am J Clin Oncol. 41:1263–1271.

Maria OM, Eliopoulos N, Muanza T. 2017. Radiation-induced oral mucositis. Front Oncol. 7:89.

Mengler L, Khmelinskii A, Diedenhofen M, Po C, Staring M, Lelieveldt BPF, Hoehn M. 2014. Brain maturation of the adolescent rat cortex and striatum: changes in volume and myelination. Neuroimage. 84: 35–44.

Nieman BJ, de Guzman AE, Gazdzinski LM, Lerch JP, Chakravarty MM, Pipitone J, Strother D, Fryer C, Bouffet E, Laughlin S, et al. 2015. White and gray matter abnormalities after cranial radiation in children and mice. Int J Radiat Oncol Biol Phys. 93:882–891.

Panagiotakos G, Alshamy G, Chan B, Abrams R, Greenberg E, Saxena A, Bradbury M, Edgar M, Gutin P, Tabar V. 2007. Long-term impact of radiation on the stem cell and oligodendrocyte precursors in the brain. PLoS One. 2:e588.

Rana P, Khan AR, Modi S, Hemanth Kumar BS, Javed S, Tripathi RP, Khushu S. 2013. Altered brain metabolism after whole body irradiation in mice: a preliminary in vivo 1H MRS study. Int J Radiat Biol. 89:212–218.

Reddy NK, Brown FC, Fogarasi MC, Yu JB, Hess J, Chiang VS. 2018. Long-term quality of life in survivors of brain metastases: a roller coaster of perspective. Cureus [Internet]. 10:e2358.

Robbins ME, Brunso-Bechtold JK, Peiffer AM, Tsien CI, Bailey JE, Marks LB. 2012. Imaging radiation-induced normal tissue injury. Radiat Res. 177:449–466.

Roman DD, Sperduto PW. 1995. Neuropsychological effects of cranial radiation: current knowledge and future directions. Int J Radiat Oncol Biol Phys. 31:983–998.

Roozendaal B, Hernandez A, Cabrera SM, Hagewoud R, Malvaez M, Stefanko DP, Haettig J, Wood MA. 2010. Membrane-associated glucocorticoid activity is necessary for modulation of long-term memory via chromatin modification. J Neurosci. 30:5037–5046.

Sabsevitz DS, Bovi JA, Leo PD, Laviolette PS, Rand SD, Mueller WM, Schultz CJ. 2013. The role of pre-treatment white matter abnormalities in developing white matter changes following whole brain radiation: a volumetric study. J Neurooncol. 114:291–297.

Schiffer WK, Mirrione MM, Dewey SL. 2007. Optimizing experimental protocols for quantitative behavioral imaging with 18F-FDG in rodents. J Nucl Med. 48:277–287.

Sun R, Zhang LY, Chen LS, Tian Y. 2016. Long-term outcome of changes in cognitive function of young rats after various/different doses of whole brain irradiation. Neurol Res. 38:647–654.

Tallet AV, Azria D, Barlesi F, Spano JP, Carpentier AF, Gonçalves A, Metellus P. 2012. Neurocognitive function impairment after whole brain radiotherapy for brain metastases: actual assessment. Radiat Oncol. 7:77.

Tofilon PJ, Fike JR. 2000. The radioresponse of the central nervous system: a dynamic process. Radiat Res. 153:357–370.

Torrens M, Malamitsi J, Karaiskos P, Valotassiou V, Laspas F, Andreou J, Stergiou C, Prassopoulos V. 2016. Although non-diagnostic between necrosis and recurrence, FDG PET/CT assists management of brain tumours after radiosurgery. In Vivo. 30:513–520.

Vállez Garcia D, Casteels C, Schwarz AJ, Dierckx R, Koole M, Doorduin J. 2015. A standardized method for the construction of tracer specific PET and SPECT rat brain templates: validation and implementation of a toolbox. PLoS One. 10:e0122363.

Vállez García D, Otte A, Dierckx R, Doorduin J. 2016. Three month follow-up of rat mild traumatic brain injury: a combined [18F]FDG and [11C]PK11195 positron emission study. J Neurotrauma. 33: 1855–1865.

Wong KP, Sha W, Zhang X, Huang SC. 2011. Effects of administration route, dietary condition, and blood glucose level on kinetics and uptake of 18F-FDG in mice. J Nucl Med. 52:800–807.

Woo SK, Lee TS, Kim KM, Kim JY, Jung JH, Kang JH, Cheon GJ, Choi CW, Lim SM. 2008. Anesthesia condition for (18)F-FDG imaging of lung metastasis tumors using small animal PET. Nucl Med Biol. 35:143–150.

Wu C, Wang C, Popescu DC, Zhu W, Somoza EA, Zhu J, Condie AG, Flask CA, Miller RH, Macklin W, et al. 2010. A novel PET marker for in vivo quantification of myelination. Bioorg Med Chem. 18: 8592–8599.

Wu C, Zhu J, Baeslack J, Zaremba A, Hecker J, Kraso J, Matthews PM, Miller RH, Wang Y. 2013. Longitudinal positron emission tomography imaging for monitoring myelin repair in the spinal cord. Ann Neurol. 74:688–698.

Zilberter Y, Zilberter M. 2017. The vicious circle of hypometabolism in neurodegenerative diseases: ways and mechanisms of metabolic correction. J Neurosci Res. 95:2217–2235.